

Discussions on the ductile fracture prediction of ship structures under impact loads

Y. Lu

State Key Laboratory of Ocean Engineering, Shanghai Jiao Tong University, Shanghai, 200240, China
Centre for Autonomous Marine Operations and Systems (AMOS), Norwegian University of Science and Technology (NTNU), Trondheim, Norway

Department of Marine Technology, Norwegian University of Science and Technology (NTNU), Trondheim, Norway

K. Liu & Z. Wang

School of Naval Architecture and Ocean Engineering, Jiangsu University of Science and Technology

W. Tang

State Key Laboratory of Ocean Engineering, Shanghai Jiao Tong University, Shanghai, 200240, China

J. Amdahl

Centre for Autonomous Marine Operations and Systems (AMOS), Norwegian University of Science and Technology (NTNU), Trondheim, Norway

Department of Marine Technology, Norwegian University of Science and Technology (NTNU), Trondheim, Norway

ABSTRACT: This study summarizes four representative failure criteria which could be applied in ship impact analysis. Robustness of these criteria are examined by simulating penetration tests of stiffened panels as well as the double hull structure. The results show that all the investigated failure criteria produce a wide scatter in ductile fracture prediction when varying mesh sizes are applied, and the predictive capacities of these criteria are variant in different validation cases. Based on it, discussions are carried out with emphasis given on the fracture mechanisms of different structural components as well as the crack propagation prediction.

1 INTRODUCTION

Growing awareness regarding marine environments provides strong incentive to develop crashworthy ship structures, preventing and reducing the risk of structural impact destruction. In evaluations of collision or grounding accidents, one of the key issues is an accurate prediction of the damage extent in ship structures. Liu et al. (2018) reviewed the calculation procedures for ship collision and grounding accidents and highlighted the importance of material fracture modelling in the development of numerical simulations.

In recent years, many ductile failure criteria have been proposed or developed. Calle and Alves (2015) classified the failure criteria commonly used in ship collision simulations into three main categories: strain based failure criteria, triaxial stress state based failure criteria and forming limit diagram based failure criteria. Among the strain based failure criteria, the equivalent plastic strain (EPS) approach is the most commonly used criterion in ship impact analysis due to its simplicity and easy implementation in finite element codes (Ehlers, 2010; Samuelides, 2015). However, this approach neglects the effect of stress states, and thus inaccurate failure strain is expected. McClintock (1968) and Rice and Tracey

(1969) carried out investigations on the evolution of cylindrical and spherical holes, and it was demonstrated that the mechanism of ductile fracture is governed by micro void nucleation, growth and coalescence. Based on it, failure criteria accounting for the influence of stress triaxiality have been developed, such as the well-known Rice-Tracey and the Cockcroft-Latham (RTCL) criterion (Toernqvist, 2003) and Johnson-Cook criterion (Johnson and Cook, 1985). However, a comprehensive study was performed by Bao and Wierzbicki (2004) and the results suggested that the effect of Lode angle on fracture prediction cannot be neglected. Since then, many advanced failure criteria which incorporate the effect of both Lode angle and stress triaxiality into the model have been developed, such as Hosford-Coulomb model (Mohr and Marcadet, 2015), modified Mohr-Coulomb (MMC) criterion (Bai and Wierzbicki, 2010). It is noted that when applied in plane stress shell elements, the effect of Lode angle in the above failure criteria is implicitly considered as stress triaxiality and Lode angle are uniquely related under this condition. In addition, many analytical models have been proposed based on the forming limit diagram to predict the necking limit of sheet metals, such as Hill criterion (Hill, 1952), Swift cri-

terion (Swift, 1952), BWH criterion (Alsos et al., 2008), M-K methods (Marciniak and Kuczyński, 1967) and so on. A detailed review can be found from Paul (2021).

In numerical simulations of ship impact analysis, FE simulated response becomes strongly mesh dependent after localized necking. Shell elements are especially vulnerable to this as there is limited resistance against thinning. Considering the onset of necking as a state of failure is a convenient way to deal with the material mesh sensitivity problem. It has been demonstrated that the forming limit diagram based failure criteria could effectively mitigate the material mesh sensitivity problem (Alsos et al., 2009). There are, however, cases where the material continues to transmit forces after the onset of necking, and thus a conservative estimation of damage extent is possibly obtained (Hogström et al., 2009). Alternatively, fracture scaling law has been regarded as another effective way to reduce mesh dependence (Ehlers et al., 2008). For the conventional fracture scaling law, it adjusts fracture strains according to varying mesh sizes based on the uniaxial tensile tests, and this approach has been applied in the calibration of EPS and RTCL criterion. Körgesaar et al. (2014) analyzed fracture behavior of shipbuilding steels subjected to different stress states, and it was demonstrated that the mesh dependency strongly depends on the stress states. Walters (2014) addressed this issue by introducing a framework which adjusts failure strain of shell elements based on both mesh size and stress triaxiality. Based on it, Körgesaar (2019) employed the MMC failure criterion and the extended Swift necking criterion in the framework to predict ductile fracture over a wide range of stress states.

In the present study, four representative failure criteria which could be applied in ship impact analysis are summarized, with special attention paid on the calibration process as well as the mesh size sensitivity. The predictive capability of these criteria for shell elements is evaluated by making comparisons with a series of indentation tests involving different materials, indenter shapes and structural arrangements. Based on these comparisons, the governing mechanisms in terms of fracture initiation as well as crack propagation are discussed in detail.

2 FRACTURE MODELLING

2.1 Ductile failure criteria

2.1.1 Equivalent plastic strain (EPS) criterion

In numerical simulations of ship collision events, a typical engineering approach to account for fracture is to define a critical equivalent plastic strain, which can be estimated from material uniaxial tensile tests.

In the approach, fracture is assumed to occur when the equivalent plastic strain reaches a critical value:

$$\varepsilon_{eq} = \sqrt{\frac{2}{3} \varepsilon_{ij}^p \varepsilon_{ij}^p} = \varepsilon_f \quad (1)$$

where ε_{ij}^p is the plastic strain tensor, and ε_{cr} is the critical equivalent plastic strain. When all through-thickness integration points satisfy the criterion, the element will be removed from the model. The Element size dependence is considered according to:

$$\varepsilon_f = \varepsilon_n + \left(\varepsilon_{f, l_e=t_e} - \varepsilon_n \right) \frac{t_e}{l_e} \quad (2)$$

where ε_n represents diffuse necking strain, and $\varepsilon_{f, l_e=t_e}$ is the failure strain under uniaxial tension state when mesh size $l_e/t_e=1$.

2.1.2 Rice-Tracey and the Cockcroft-Latham (RTCL) criterion

Toernqvist (2003) developed the RTCL criterion by combining two well-known fracture models, i.e., the Rice Tracey and the Cockcroft Latham criteria, in order to cover a wide range of stress triaxialities. In the model, D is the integral function of damage, which can be expressed as:

$$D = \frac{1}{\varepsilon_f} \int f(\eta) d\varepsilon \quad (3)$$

where ε_n is failure strain obtained from uniaxial tensile test, $d\varepsilon$ is the effective plastic strain increment, $f(\eta)$ is given as:

$$f(\eta) = \begin{cases} 0 & \eta \leq -1/3 \\ 2 \frac{1 + \eta \sqrt{12 - 27\eta^2}}{3\eta + \sqrt{12 - 27\eta^2}} & -1/3 \leq \eta \leq 1/3 \\ \frac{1}{1.65} \exp(3/2\eta) & \eta \geq 1/3 \end{cases} \quad (4)$$

where η represents the stress triaxiality which is typically defined as the ratio of hydrostatic stress and equivalent Von Mises stress: The elements will be removed once all thickness integration points satisfy the condition $D \geq 1$.

Similarly, when different mesh sizes are applied, critical strain in RTCL criterion is scaled in accordance with the relation in Eq. (2).

2.1.3 Bressan-Williams-Hill (BWH) criterion

The stress-based forming limit diagram has been proved to be effective when dealing with complex loading paths. Alsos et al. (2008) developed a stress based necking criterion called BWH criterion by

combining Hill necking criterion (Hill, 1952) with Bressan and Williams shear stress criterion (Bressan and Williams, 1983). It can be expressed in terms of principal strain ratio as:

$$\sigma_1 = \begin{cases} \frac{2K}{\sqrt{3}} \frac{1 + \frac{1}{2}\alpha}{\sqrt{\alpha^2 + \alpha + 1}} \left(\frac{2}{\sqrt{3}} \frac{\tilde{n}}{1 + \alpha} \sqrt{\alpha^2 + \alpha + 1} \right)^n & \alpha \leq 0 \\ \frac{2K}{\sqrt{3}} \frac{\left(\frac{2}{\sqrt{3}} \tilde{n} \right)^n}{\sqrt{1 - \left(\frac{\alpha}{2 + \alpha} \right)^2}} & \alpha > 0 \end{cases} \quad (5)$$

where α is the ratio between major principal strain rate and minor principal strain rate. K , n are the material parameters in power law relation. BWH criterion assumes the onset of necking as a state of failure, and therefore the mesh size sensitivity can be reduced. When applied in FE models, the criterion is activated by checking failure in the mid through-thickness integration point of shell elements.

2.1.4 Fracture strain scaling based on stress state and mesh size (2FS-ex) criterion

Walters (2014) proposed a general framework which adjusts failure strain of shell elements based on both mesh sizes and stress states in order to reduce mesh size sensitivity. Based on it, Kõrgesaar (2019) employed the MMC plane stress criterion and the extended Swift necking criterion in the framework to predict the fracture behavior in ship impact analysis. This approach is denoted as 2FS-ex criterion. In the fracture scaling framework, it is assumed that the element is removed when all the integration points satisfy the criterion, and the failure strain is obtained through:

$$\varepsilon_f(\eta, t_e/l_e) = \varepsilon_n(\eta) + (\varepsilon_{f,cal}(\eta) - \varepsilon_n(\eta)) \frac{t_e}{l_e} \quad (6)$$

where $\varepsilon_{f,cal}(\eta)$ is the calibration function depending on the upper bound $\varepsilon_{f,MMC}(\eta)$ and lower bound $\varepsilon_n(\eta)$, which can be expressed as:

$$\varepsilon_{f,cal}(\eta) = \varepsilon_n(\eta) + (\varepsilon_{f,MMC}(\eta) - \varepsilon_n(\eta)) \frac{L_{e,cal}}{t_{e,cal}} \quad (7)$$

$\varepsilon_{f,MMC}(\eta)$ is the plane stress MMC fracture model. Under the proportional loading path, it can be expressed as:

$$\varepsilon_{MMC} = \left\{ \frac{K}{C_2} f_3 \left[\sqrt{\frac{1 + C_1^2}{3}} f_1 + C_1 \left(\eta + \frac{f_2}{3} \right) \right] \right\}^{-\frac{1}{n}} \quad (8)$$

Where f_1, f_2, f_3 is given as:

$$\begin{aligned} f_1 &= \cos \left\{ \frac{1}{3} \arcsin \left[\frac{-27}{2} \eta \left(\eta^2 - \frac{1}{3} \right) \right] \right\} \\ f_2 &= \sin \left\{ \frac{1}{3} \arcsin \left[\frac{-27}{2} \eta \left(\eta^2 - \frac{1}{3} \right) \right] \right\} \\ f_3 &= C_3 + \frac{\sqrt{3}}{2 - \sqrt{3}} (1 - C_3) + \left(\frac{1}{f_1} - 1 \right) \end{aligned} \quad (9)$$

C_1, C_2 and C_3 are the material constants governing the fracture process. When modeling ductile fracture for non-proportional loading paths, a damage accumulation rule is introduced. It is expressed as:

$$D = \int_0^{\bar{\varepsilon}_p} \frac{1}{\varepsilon_{MMC}(\eta)} d\bar{\varepsilon}_p \quad (10)$$

where $d\bar{\varepsilon}_p$ represents the increment of plastic strain.

$\varepsilon_n(\eta)$ is represented as Swift diffuse necking criterion with extension where necking strain in low stress triaxiality equals to necking strain in uniaxial tension state. The Swift diffuse necking can be expressed as:

$$\varepsilon_1 = \frac{2(2 - \beta)(1 - \beta + \beta^2)}{4 - 3\beta - 3\beta^2 + 4\beta^3} n \quad (11)$$

$$\varepsilon_2 = \frac{2(2\beta - 1)(1 - \beta + \beta^2)}{4 - 3\beta - 3\beta^2 + 4\beta^3} n \quad (12)$$

Where power law exponent n is equal to uniform elongation.

2.2 Summary of the failure criteria

In order to have a better understanding of the characteristics of the above failure criteria, fracture loci of the failure criteria are represented in the space of stress triaxiality and equivalent plastic strain under the assumption of proportional loading, as shown in Figure 1. The example calibration parameters in the failure criteria are determined from tensile tests on standard structural steel S235JR for mesh size $l_e/t_e=1$ (Kõrgesaar et al., 2018), as summarized in Table 1. It is noted that the fracture strain at uniaxial tension determined from the 2FS-ex criterion is slightly larger than the one from EPS and RTCL criteria. This is because the fracture strain for mesh size $l_e/t_e=1$ in 2FS-ex criterion is obtained from the scaling in Eq. (7) instead of the simulations of tensile tests, and thus slight differences between uniaxial fracture strain are expected.

As shown in Figure 1, a constant fracture strain is obtained for different stress states when applying EPS criterion. In contrast, the fracture locus obtained from the RTCL criterion exhibits a monotonic decrease when the stress triaxiality increases due to the incorporation of the hydrostatic stress effect in the model. For BWH criterion, it is converted into equivalent plastic strain space under the assumption of proportion loading path. It is obvious that a conservative estimation of fracture strain is obtained from the BWH criterion as the energy dissipation in the post necking region is omitted. In addition, this approach is valid for multi-axial tension domain, in which the stress triaxiality ranges from uniaxial tension to equi-biaxial tension state. In contrast to the other criteria, the influence of Lode angle is implicitly incorporated in 2FS-ex model. It is evident from Figure 1 that the equivalent plastic strain to fracture in pure shear is lower than that in uniaxial tension, and the fracture strain increases from plane strain to equi-biaxial tension state. This conclusion is consistent with the experimental results reported by Bao and Wierzbicki (2004) due to the implicit incorporation of the Lode angle dependence in the model. However, the calibration process of 2FS-ex criterion is not straightforward as three fracture parameters are involved in the model, which means at least three material tests are required.

It is acknowledged that a well-constructed failure criterion should not only capture the main physical mechanism of ductile fracture, but also could be easily interpreted by practitioner in industrial analysis. In the next sections, prediction accuracy of the above failure criteria will be further discussed by making comparisons for a series of penetration tests.

Table 1 Calibration parameters in different failure criteria from tensile tests

Failure criteria	Calibration parameters in the model
EPS criterion	$\epsilon_f=0.479$
RTCL criterion	$\epsilon_f=0.479$
BWH criterion	$n=0.21$
2FS-ex criterion	$c_1=0.0271$, $c_2=353.49$, and $c_3=0.995$ when $L_{e,cal}/t_{e,cal}=1/6$

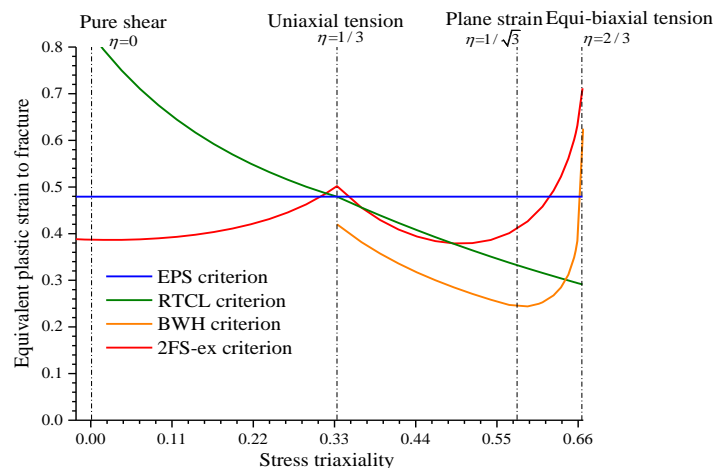


Figure 1 Examples of fracture loci of four failure criteria in the space of stress triaxiality and equivalent plastic strain

3 NUMERICAL VALIDATIONS WITH INDENTATION TESTS

In this section, three quasi-static impact experiments are examined to evaluate the performance of different failure criteria in prediction of ductile fracture behavior of ship structures.

The computations are carried out with the explicit finite element package LS-DYNA. In all simulations, the specimens are modeled by four-node shell elements with five-integration points through the thickness. The ductile failure criteria, along with the elasto-plastic flow model, are implemented in the finite element code through a user-defined material subroutine. The calibration parameters in EPS, RTCL and BWH criterion are determined from numerical simulations of the uniaxial tensile tests for the target materials, while the test data from Korge-saar et al. (2018) are utilized to identify the parameters in 2FS-ex criterion for all simulations as the available material test data in the penetration tests are limited. For the indenter, a rigid material (Mat.020-Rigid) is employed to ensure no deformation. The contact between the striker and the specimen is defined as ‘Automatic Surface to Surface’, and the hourglass control based on the viscosity stresses is added to physical stresses at local element level in order to suppress the hourglass modes.

3.1 Indentation tests on stiffened panels with different configurations

A series of panel indentation experiments were carried out by Alsos and Amdahl (2009). Herein, two different configurations of stiffened panels are considered for validation purposes: stiffened panel with one flat bar (1-FB) and two flat bars (2-FB), as shown in Figure 2(a). The specimen is welded to a strong frame, which consists of four massive steel boxes assembled by welding. Figure 2(b) shows the experimental setup. The cone-shaped indenter with a spherical nose was forced to penetrate through the center of the plates with a velocity of 10 mm/min. The plates and flat bar stiffeners are made from mild steel (S235JR EN10025), whereas the frames are made from high strength steel (S355NH EN10210). The properties of the materials reported by Alsos et al. (2009) are utilized. See Table 2. Mesh sizes in the impact zones could be refined enough to track local deformation. Herein, three different mesh sizes are employed, i.e., 5mm, 10 mm and 18 mm, corresponding to $l_e/t_e=1, 2, 3.6$ with respect to the plate thickness. Figure 2(c) illustrates the finite element models of the specimens with 10 mm mesh sizes.

ment. The ratios between the numerical and experimental dissipated energy (E_{sim}/E_{exp}) for the validation cases with varying mesh sizes are presented in Figures 5-7 along with the deviations of 20% with red dash lines.

It is found that scatter exists in all cases when different failure criteria are applied. In 1-FB and 2-FB cases where stiffened panels are indented by a spherical nose indenter, 2FS-ex criterion achieves a better correlation with the test results with deviations being within 20%. For EPS and RTCL criterion, a scatter is noticed when different mesh sizes are applied. This may be associated with the fracture scaling law in the two models where fracture strains for different mesh sizes are determined from uniaxial tensile test only, and thus the dependence of the mesh size sensitivity on the stress states are neglected. As pointed by K orgesaar et al. (2014), the fracture strain is more sensitive to the mesh size in uniaxial tension than in the plane strain and biaxial tension state. To further confirm this, the evolution of stress triaxiality for the through-thickness integration points with mesh $l_e/t_e=1$ for EPS criterion is shown in Figure 8. As can be seen, the stress states of the failed elements in 1-FB and 2-FB specimen are close to plane strain tension, and the stress states of three integration points are identical after the initial oscillation caused by contact between indenter and specimen, indicating stretching dominant mode. In contrast, the averaged stress triaxiality for the failed element in 2-FB specimen is closer to uniaxial tension state, and this explains why the scatter in 1-FB specimen is larger than that in 2-FB specimen for EPS and RTCL. For BWH model, it tends to generate conservative results in terms of fracture initiation of the specimens. A significant scatter is also observed with varying mesh sizes, while coarse meshes tend to provide better estimation in terms of dissipated energies.

The situation changes when different indenters are considered in the indentation tests. Fracture of Knife edge and Flat edge specimens involves not only fracture initiation, but also significant crack propagation process. The normalized displacements corresponding to fracture initiation from different failure criteria are summarized in Table 5. It is observed that the performance of the failure criteria in predicting fracture initiation of the Knife edge specimen is not as accurate as that of the Flat edge specimen. RTCL and 2FS-ex criteria exhibit good correlations with the test results of the Flat edge specimen, while for the Knife edge specimen, BWH exhibits a better correlation with the test results although the fine mesh predicts the fracture initiation earlier. This is because the initial crack in the Knife edge specimen is a very local phenomenon, which is more difficult to detect in the finite element models. Consequently, fracture initiation predicted by relatively large mesh sized models tends to be delayed.

As the indentation progresses, cracks propagate along the specimens until the reaction force drops. Discrepancies are apparent for both the Knife edge and the Flat edge specimens, especially for the EPS criterion where larger dissipated energy are obtained. This may be motivated by the fact that fracture strain for crack propagation is lower than that obtained from tensile tests. This finding is consistent with the results of Cerup-Simonsen et al. (2009) where a crack propagation criterion is established and compared with the failure initiation criterion. Furthermore, the removal of fractured elements in the FE simulations cannot adequately capture the large stresses developed around fractured areas, and this issue may become worse when coarse mesh sizes are applied.

Figure 9 shows the final deformation shapes of Knife edge specimen from the test and EPS criterion. Coarsely meshed models cannot adequately replicate the crack propagation path in the test. Attempts have been made to deal with this problem by coupling of the constitutive model and fracture model, for example, continuum damage mechanics approach developed by Chaboche (1988a, b) and Lemaitre and Desmorat (2005), while calibration process of these models is complex, which significantly limits their applications in ship impact analysis. In the future, failure criteria that are capable of covering both fracture initiation and propagation in practical engineering problems should be investigated.

For the case of double hull structure, the calibrated EPS criterion is found to provide a better estimation of ductile fracture, and it is relatively mesh size insensitive. In comparison, the RTCL criterion tends to predict fracture earlier, hence generating more conservative results when compared with the test results. This discrepancy is expected as the fracture strain in the RTCL model exhibits a monotonic function in terms of the stress triaxiality, as shown in Figure 1. Consequently, when predicting ductile fracture of the plate members where stress states are confined in multi-axial regime, the critical fracture strain is relatively low. For BWH and 2FS-ex criterion, it is apparent that the delay of failure prediction exists in the numerical models, which results in larger dissipated energies than the real ones. The major causes of the discrepancy in BWH criterion may be attributed to the overlook of fracture prediction in low stress triaxiality region.

Figure 10 shows the loading paths of three elements in the outer stiffeners in fine mesh sized model. For Element 1, the stress state is mainly limited in the region between pure shear and uniaxial tension state during the deformation process, while erosion does not take place in the element as BWH criterion is not involved in this region. In general, BWH criterion searches for the localized necking in the material. However, no preceding strain localiza-

tion occurs during low stress triaxialities. It is noticed that the loading path of Element 2 exceeds BWH locus at the time step before fracture initiation. This can be expected as the loading path of Element 2 is not proportional, and thus necking condition is probably not satisfied when plastic strain reaches the limit strain. Additionally, differences in the prediction results from 2FS-ex criterion may lie in inaccurate parameter identification for the target material. The calibrated parameters in 2FS-ex criterion are determined from the material tests on S235JR steel, in which material properties are not identical with that of the material used to manufacture the double hull structure. For the material in the double hull structure, the diffuse necking strain is significantly lower than that of S235JR steel, where fracture strain in large shell element, i.e., $\epsilon_f = 0.29$, is considered as the diffuse necking strain. Thus, when inaccurately calibrated 2FS-ex criterion is applied, the predicted dissipated energy is obviously overestimated. Therefore, it is necessary to perform a series of material tests on specific shipbuilding steel before 2FS-ex criterion is applied in the impact analysis of ship structures.

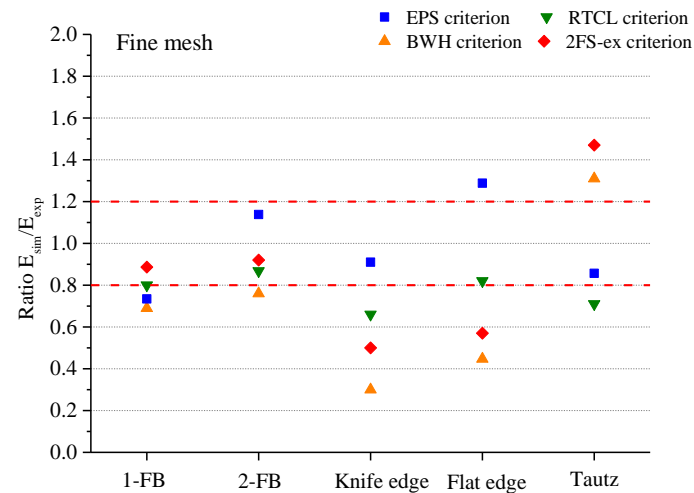


Figure 5 Normalized energy for all the indentation tests with the finest mesh sizes

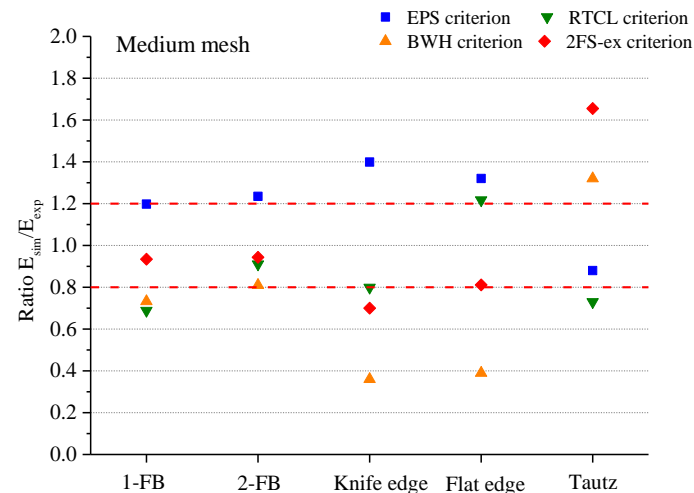


Figure 6 Normalized energy for all the impact tests with the medium mesh sizes

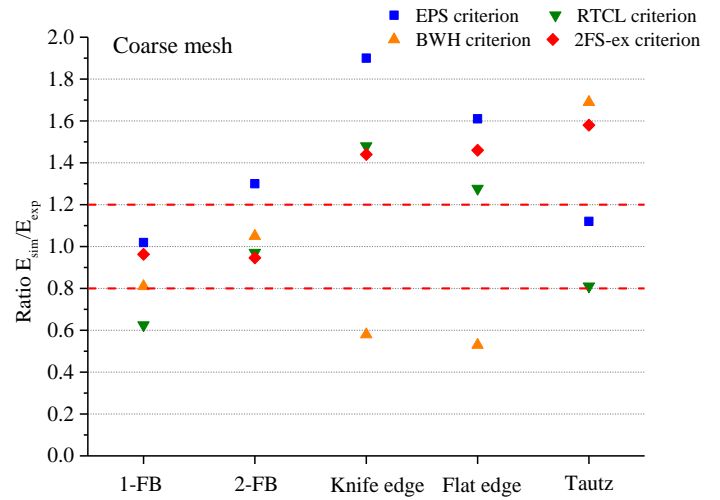


Figure 7 Normalized energy for all the impact tests with the coarse mesh sizes

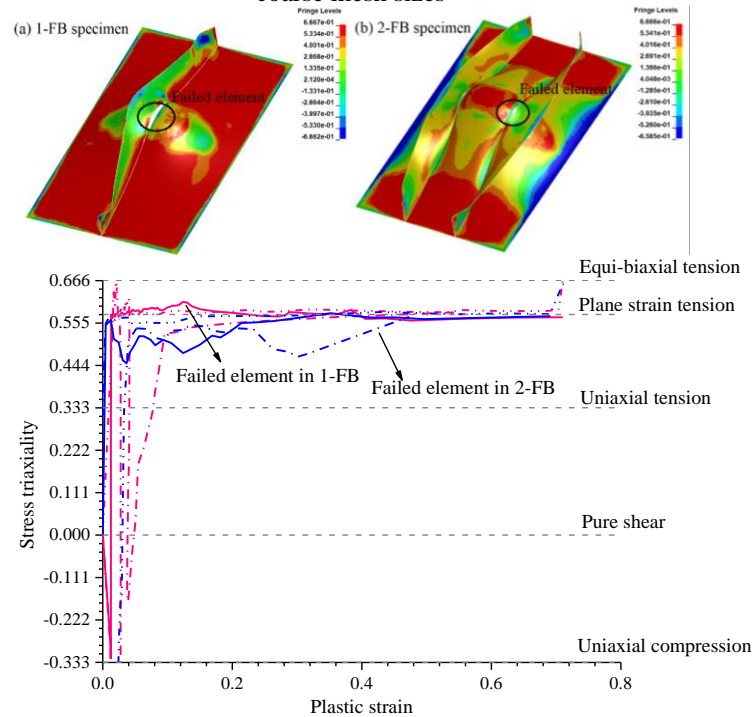
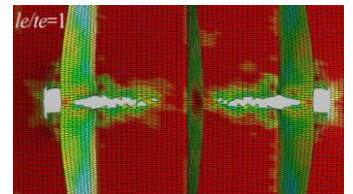
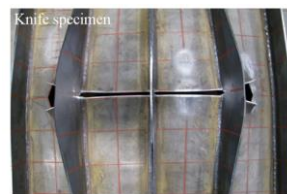


Figure 8 Post fracture initiation shapes for 5 mm mesh sizes with contours of stress triaxiality along with the evolution of stress triaxiality for the first failed elements

Table 5 Normalized displacements corresponding to fracture initiation from different failure criteria

D_{sim}/D_{exp}	Knife edge specimen			Flat edge specimen		
	$l_e/t_e=1$	$l_e/t_e=2$	$l_e/t_e=3$	$l_e/t_e=1$	$l_e/t_e=2$	$l_e/t_e=3$
EPS	1.60	1.57	1.71	1.38	1.05	1.18
RTCL	1.50	1.52	1.60	1.08	0.9	0.93
BWH	0.55	0.81	0.86	0.93	0.78	0.98
2FX-ex	1.05	1.35	1.57	0.95	0.93	1.11



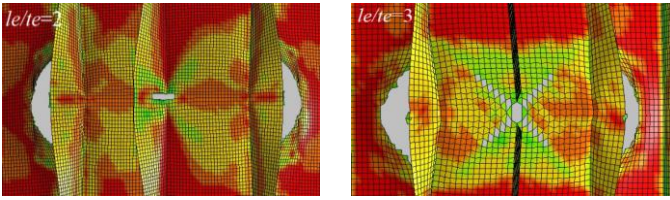


Figure 9 Deformation shapes of Knife edge and Flat edge specimens in the test and FE models from EPS criterion

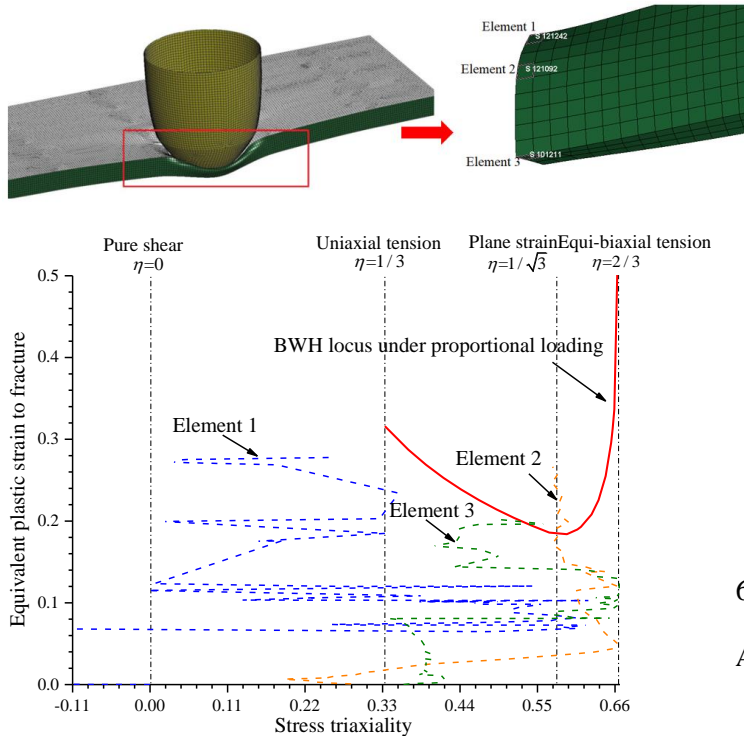


Figure 10 Loading paths of elements in stiffeners for mesh size $le/te=4$ along with fracture locus of BWH criterion

5 CONCLUSIONS

This study discusses the performance of four representative failure criteria in predicting fracture behavior of ship structures under impact loads. Numerical validations with different indentation tests are carried out. Based on the simulation results, the predictive capacity of these criteria in terms of dissipated energy is assessed. The major conclusions from the present study are summarized as follows:

- The EPS and the RTCL criterion provide accurate estimates of ductile fracture initiation when large dimensions of ship structures are involved, while the fracture scaling method established for the two models produces a scatter as the effect of stress state on mesh size dependency is neglected.
- When coarse mesh sizes are applied, the BWH criterion is a reliable approach to predict ductile fracture initiation, while conservative results are mostly obtained when finely meshed models are involved. Additionally, the capacity of the BWH criterion to predict shear fracture is proved to be limited.

- 2FS-ex criterion yields good estimation of fracture initiation when different mesh sizes are employed, but the calibration process of the criterion is not straightforward as at least three material tests with the target material are required. It is demonstrated that incorrect parameters in the criterion would lead to significant deviations in the prediction results.
- The predictive capabilities of all the investigated criteria regarding crack propagation are not accurate enough, especially when coarse mesh sizes are involved. Therefore, criteria for prediction of fracture initiation as well as propagation in ship structures should be further investigated.
- The present study focuses on quasi-static impact cases, and the strain rate effect on the fracture prediction is not accounted for. In the future study, rate dependence factor should be incorporated in the fracture model to give a more precise prediction of ship structures in collision and grounding events.

6 REFERENCES

- Alsos, H.S., Amdahl, J. 2009. On the resistance to penetration of stiffened plates, Part I – Experiments. *International Journal of Impact Engineering* 36 (6), 799-807.
- Alsos, H.S., Amdahl, J., Hopperstad, O.S. 2009. On the resistance to penetration of stiffened plates, Part II: Numerical analysis. *International Journal of Impact Engineering* 36 (7), 875-887.
- Alsos, H.S., Hopperstad, O.S., Törnqvist, R., Amdahl, J. 2008. Analytical and numerical analysis of sheet metal instability using a stress based criterion. *International Journal of Solids and Structures* 45 (7), 2042-2055.
- Bai, Y., Wierzbicki, T. 2010. Application of extended Mohr–Coulomb criterion to ductile fracture. *International Journal of Fracture* 161 (1), p.1-20.
- Bao, Y., Wierzbicki, T. 2004. On fracture locus in the equivalent strain and stress triaxiality space. *International Journal of Mechanical Sciences* 46 (1), 81-98.
- Bressan, J.D., Williams, J.A. 1983. The use of a shear instability criterion to predict local necking in sheet metal deformation. *International Journal of Mechanical Sciences* 25 (3), 155-168.
- Calle, M.A.G., Alves, M. 2015. A review-analysis on material failure modeling in ship collision. *Ocean Engineering* 106, 20-38.
- Cerup-Simonsen, B., Törnqvist, R., Lützen, M. 2009. A simplified grounding damage prediction method and its application in modern damage stability requirements. *Marine Structures* 22 (1), 62-83.
- Chaboche, J. 1988a. Continuum Damage Mechanics: Part I--- General Concepts. *Journal of Applied Mechanics* 55.
- Chaboche, J. 1988b. Continuum Damage Mechanics: Part II— Damage Growth, Crack Initiation, and Crack Growth. *Journal of Applied Mechanics-transactions of The Asme - J APPL MECH* 55.
- Ehlers, S. 2010. The influence of the material relation on the accuracy of collision simulations. *Marine Structures* 23 (4), 462-474.

- Ehlers, S., Broekhuijsen, J., Alsos, H.S., Biehl, F., Tabri, K. 2008. Simulating the collision response of ship side structures: a failure criteria benchmark study. *International Shipbuilding Progress* 55 (1-2), 127-144.
- Hill, R. 1952. On discontinuous plastic states, with special reference to localized necking in thin sheets. *Journal of the Mechanics & Physics of Solids* 1 (1), 19-30.
- Hogström, P., Ringsberg, J.W., Johnson, E. 2009. An experimental and numerical study of the effects of length scale and strain state on the necking and fracture behaviours in sheet metals. *International Journal of Impact Engineering* 36 (10), 1194-1203.
- Johnson, G.R., Cook, W.H. 1985. Fracture characteristics of three metals subjected to various strains, strain rates, temperatures and pressures. *Engineering Fracture Mechanics* 21 (1), 31-48.
- Körgeaar, M. 2019. The effect of low stress triaxialities and deformation paths on ductile fracture simulations of large shell structures. *Marine Structures* 63, 45-64.
- Körgeaar, M., Remes, H., Romanoff, J. 2014. Size dependent response of large shell elements under in-plane tensile loading. *International Journal of Solids and Structures* 51 (21), 3752-3761.
- Körgeaar, M., Romanoff, J., Remes, H., Palokangas, P. 2018. Experimental and numerical penetration response of laser-welded stiffened panels. *International Journal of Impact Engineering* 114, 78-92.
- Lemaitre, J., Desmorat, R. 2005. Engineering Damage Mechanics Creep, Creep-Fatigue, and Dynamic Failures. *Springer Berlin Heidelberg*.
- Liu, B., Pedersen, P.T., Zhu, L., Zhang, S. 2018. Review of experiments and calculation procedures for ship collision and grounding damage. *Marine Structures* 59 (5), 105-121.
- Marciniak, Z., Kuczyński, K. 1967. Limit strains in the processes of stretch-forming sheet metal. *International Journal of Mechanical Sciences* 9 (9), 609,IN601,613-612,IN602,620.
- McClintock, F.A. 1968. A Criterion for Ductile Fracture by the Growth of Holes. *Journal of Applied Mechanics* 35 (2), 363-371.
- Mohr, D., Marcadet, S.J. 2015. Micromechanically-motivated phenomenological Hosford–Coulomb model for predicting ductile fracture initiation at low stress triaxialities. *International Journal of Solids and Structures* 67-68, 40-55.
- Paul, S.K. 2021. Controlling factors of forming limit curve: A review. *Advances in Industrial and Manufacturing Engineering* 2, 100033.
- Rice, J.R., Tracey, D.M. 1969. On the ductile enlargement of voids in triaxial stress fields*. *Journal of the Mechanics and Physics of Solids* 17 (3), 201-217.
- Samuelides, M. 2015. Recent advances and future trends in structural crashworthiness of ship structures subjected to impact loads. *Ships and Offshore Structures* 10 (5), 488-497.
- Stoughton, T.B., Zhu, X. 2004. Review of theoretical models of the strain-based FLD and their relevance to the stress-based FLD. *International Journal of Plasticity* 20 (8-9), 1463-1486.
- Swift, H.W. 1952. Plastic instability under plane stress. *Journal of the Mechanics and Physics of Solids* 1 (1), 1-18.
- Tautz, I., Schöttelndreyer, M., Lehmann, E., Fricke, W. 2013. Collision tests with rigid and deformable bulbous bows driven against double hull side structures. *International conference of Collision and Grounding of Ships and Offshore Structures*.
- Toernqvist, R. 2003. Design of Crashworthy Ship Structures.
- Villavicencio, R. 2012. Response of ship structural components to impact loading. *IST Lisbon (Portugal)*.
- Walters, C.L. 2014. Framework for adjusting for both stress triaxiality and mesh size effect for failure of metals in shell structures. *International Journal of Crashworthiness* 19 (1), 1-12.